Photoluminescence

Deutsche Ausgabe: DOI: 10.1002/ange.201601191
Internationale Ausgabe: DOI: 10.1002/anie.201601191

Unconventional Luminescent Centers in Metastable Phases Created by Topochemical Reduction Reactions

*Bo-Mei Liu, Zhi-Gang Zhang, Kai Zhang, Yoshihiro Kuroiwa, Chikako Moriyoshi, Hui-Mei Yu, Chao Li, Li-Rong Zheng, Li-Na Li, Guang Yang, Yang Zhou, Yong-Zheng Fang, Jing-Shan Hou, Yoshitaka Matsushita, and Hong-Tao Sun**

Abstract: *A low-temperature topochemical reduction strategy is used herein to prepare unconventional phosphors with luminescence covering the biological and/or telecommunications optical windows. This approach is demonstrated by using Bi^{III}-doped Y_2O_3 ($Y_{2-x}Bi_xO_3$) as a model system. Experimental results suggest that topochemical treatment of $Y_{2-x}Bi_xO_3$ using CaH_2 creates randomly distributed oxygen vacancies in the matrix, resulting in the change of the oxidation states of Bi to lower oxidation states. The change of the Bi coordination environments from the [BiO_6] octahedra in $Y_{2-x}Bi_xO_3$ to the oxygen-deficient [BiO_{6-z}] polyhedra in reduced phases leads to a shift of the emission maximum from the visible to the near-infrared region. The generality of this approach was further demonstrated with other phosphors. Our findings suggest that this strategy can be used to explore Bi-doped or other classes of luminescent systems, thus opening up new avenues to develop novel optical materials.*

The development of functional materials has long benefited from advances in synthetic strategies. As is well known, conventional high-temperature synthetic routes can be used to prepare a broad spectrum of complex oxides with thermodynamically stable phases, precluding the formation of metastable materials. In marked contrast, low-temperature topochemical reduction reactions have allowed the preparation of complex transition-metal-oxide phases bearing highly unusual oxidation states and coordination geometries, attracting tremendous attention in the field of solid-state chemistry.[1–19] The principle advantage of this "soft" chemical route lies in the fact that it is driven by kinetics, thus allowing rational design of structures and compositions as metastable products at considerably lower reaction temperatures than when conventional techniques are used. To date, a series of material systems, such as $LaNiO_2$, $SrFeO_2$, $LaSrCoO_3H_{0.7}$, and $BaTiO_{3-x}H_x$, have been prepared through this route.[1–19] Previous efforts have focused on the investigation of magnetic compounds containing transition-metal ions,[1–17,19] and little attention has been paid to materials containing rare-earth ions.[18] As far as we are aware, the use of topochemical reaction for the controlled synthesis of functional materials containing heavier p-block metal ions has never been explored.

Novel luminescent materials emitting in the near-infrared (NIR) spectral region are urgently needed in connection with applications for bioimaging and telecommunications. Luminescent materials containing bismuth, one of the most investigated p-block elements, have attracted significant research interest owing to their importance in both fundamental science and practical applications for solid-state lighting, bioimaging, lasers, amplifiers, and detectors.[20–24] The complex photophysical behaviors exhibited by various Bi-containing material systems can be attributed to the diverse range of oxidation states available to Bi and to its propensity to form molecular clusters.[21] Interestingly, it has been found that some material systems containing Bi show ultrawide NIR photoluminescence (PL). However, rational syntheses of such systems remain elusive, although some NIR emitters can be stabilized by Lewis acids or exist in molecular crystals that were synthesized by wet-chemistry routes.[22h] Therefore, it is highly desirable to develop novel generic approaches to create unconventional Bi-based emitters, which will not only improve the designability of this class of

[*] B.-M. Liu, Y. Zhou, Prof. Dr. H.-T. Sun
College of Chemistry, Chemical Engineering and Materials Science
Soochow University, Suzhou 215123 (P.R. China)
E-mail: timothyhsun@gmail.com
Z.-G. Zhang, Prof. Dr. Y. Kuroiwa, Prof. Dr. C. Moriyoshi
Department of Physical Science, Hiroshima University
Higashihiroshima, Hiroshima 739-8526 (Japan)
K. Zhang, Prof. Dr. Y.-Z. Fang, Dr. J.-S. Hou
School of Materials Science and Engineering
Shanghai Institute of Technology, Shanghai 201418 (P.R. China)
Prof. Dr. H.-M. Yu
Shanghai Institute of Ceramics, Chinese Academy of Sciences
Shanghai 200050 (P.R. China)
C. Li, Prof. Dr. G. Yang
Electronic Materials Research Laboratory, Key Laboratory of the Ministry of Education and International Center for Dielectric Research, Xi'an Jiaotong University, Xi'an 710049 (P.R. China)
Dr. L.-R. Zheng
Beijing Synchrotron Radiation Facility
Institute of High Energy Physics
Chinese Academy of Sciences
Beijing 100049 (P.R. China)
Prof. Dr. L.-N. Li
Shanghai Synchrotron Radiation Facility
Shanghai Institute of Applied Physics
Chinese Academy of Sciences
Shanghai 201204 (P.R. China)
Dr. Y. Matsushita
National Institute for Material Sciences (NIMS)
1-2-1 Sengen, Tsukuba-city, Ibaraki 305-0047 (Japan)

Supporting information for this article can be found under: http://dx.doi.org/10.1002/anie.201601191.

materials, but also extend their practical applications in biomedicine and photonics.

Herein, we show that the low-temperature topochemical reduction route can be adopted as a generic strategy to develop unconventional emitters stabilized by metastable phases. This strategy is first demonstrated using Bi^{3+}-doped Y_2O_3 ($Y_{1.992}Bi_{0.008}O_3$) as a precursor. Topochemical reduction of $Y_{1.992}Bi_{0.008}O_3$ yields an oxygen-deficient oxide, resulting in a change in the coordination environment of Bi from that in the $[BiO_6]$ octahedra in $Y_{1.992}Bi_{0.008}O_3$ to that in $[BiO_{6-z}]$ ($z<6$) polyhedra in reduced phases. That is, after this reduction process, Bi centers exist in lower oxidation states than commonly observed for Bi species. The combination of structural and spectroscopic analyses allows us to correlate low-valence Bi in the $[BiO_{6-z}]$ polyhedra with the emergence of NIR PL. Finally, we demonstrate the sufficient generality of this strategy with other oxide phosphors, including Bi-doped $LaGaO_3$, La_2O_3, and $LaAlO_3$.

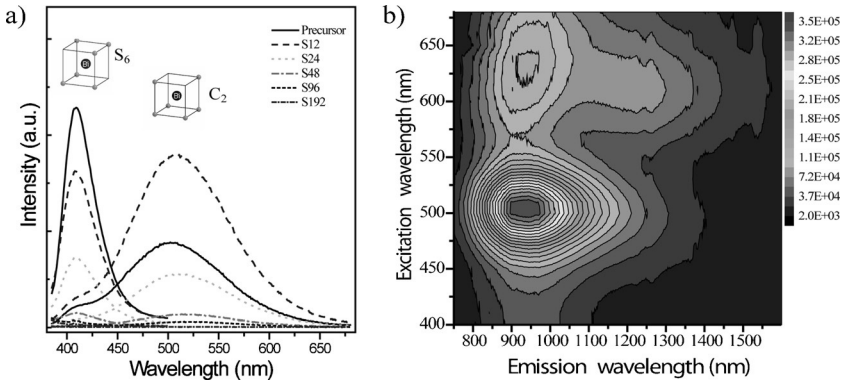

Figure 1. a) PL spectra of the precursor and reduced phases upon excitation at $\lambda = 324$ and 371 nm, respectively. Inset: the Bi ions situated at the S_6- and C_2-symmetric sites. b) 2D excitation–emission graph of the S48 sample showing the band maxima at different excitation wavelengths. For example, excitation at $\lambda = 498$ nm leads to an emission maxima occurring at circa 940 nm with a relative emission intensity of 35 000. See Figure S 7 a,b for the corresponding emission spectra and Figure S6 for color versions of 2D excitation–emission graphs for samples S12, S24, S96, and S192.

The topochemical reduction of $Y_{1.992}Bi_{0.008}O_3$ was achieved using CaH_2 as a solid-state reducing agent, resulting in a white to yellow compound depending on the harshness of the reaction conditions employed (see Figure S1 and the experimental details in the Supporting Information). The samples were denoted S*t*, where *t* represents the treatment duration in hours. The ICP-MS analysis revealed that the ratio of Bi/(Y + Bi) is circa 0.4 % and a very small amount of Ca (0.11 wt %) was left in the final products. Thermogravimetric MS measurements show the absence of hydrogen in the reduced phases, and the emergence of a signal attributable to CO_2^+ suggests the existence of $CaCO_3$ and/or $Ca(HCO_3)_2$ byproducts (Figure S2). It was found that the samples thermally treated in air could convert back into the white precursor (Figure S3). We thus collected the thermogravimetric data by heating the reduced phases in flowing oxygen for the evaluation of their oxygen content (Figure S4). Note that owing to the presence of calcium-related byproducts, the lightly reduced products, for example, the S12 and S24 samples, do not show any weight increase. Further extension of the treatment duration leads to a noticeable weight increase from circa 550 °C. Assuming that the S12 sample does not have any oxygen vacancies and that the byproducts are identical in all samples, we could roughly deduce the oxygen stoichiometry within the reduced phases (Table S1). Energy-dispersive X-ray spectroscopy (EDS) mapping of Y, O, and Bi contents confirmed that the elements are homogenously distributed in the matrix. Furthermore, the electron diffraction pattern shows no signs of superstructure, implying that oxygen vacancies are randomly distributed in the matrices (Figure S5).

Figure 1 a displays the PL spectra of the $Y_{1.992}Bi_{0.008}O_3$ precursor after excitation at $\lambda = 371$ and 324 nm, which show emission band maxima at circa $\lambda = 410$ and 502 nm, respectively. Experimental and theoretical results have revealed that Bi^{3+} ions in the S_6- and C_2-symmetric sites in the yttria contribute to these emission bands.[24] It is found that with the increase in the treatment duration from 12 h to 192 h, the PL intensity derived from both active centers slowly decreases and these emission bands disappear totally for the S192 sample. Interestingly, this change is accompanied by the occurrence of new emission bands at wavelengths greater than $\lambda = 700$ nm (Figure 1 b; Figure S6, S7). It is noteworthy that the undoped Y_2O_3 undergoing the same treatment process is PL-inactive, implying that the NIR PL is not derived from structural defects of yttria, but is instead closely connected to the Bi ions.

To gain more insight into the mechanism of the PL evolution, we took high-resolution synchrotron X-ray diffraction (XRD) measurements for the typical products (Figure 2; Figure S8). All of these samples exhibit a cubic structure with the space group $Ia\bar{3}$, and no extra diffraction lines are detected. Crystal structure refinement by the Rietveld method has been performed using the software package GSAS (general structure analysis system).[25] It is assumed that Bi ions are randomly situated at the Y position. For all samples, we set the occupation factors of Y and Bi at 0.996 and 0.004, respectively. Rietveld refinement for the reduced samples was carried out by first refining the background, cell parameters, pseudo-Voigt peak profile coefficients, atomic coordinates, and displacement parameters for all atoms, and then refining the occupancy of oxygen. We found that the precursor and the S48 and S192 samples have similar cell parameters, bond lengths, and angles, suggesting that the structure of yttria is not strongly influenced by the oxygen extraction (Table S2–S4). Furthermore, such a refinement process leads to an excellent convergence, yielding the stoichiometric compositions of $Y_{1.992}Bi_{0.008}O_{2.95}$ ($R_{wp} = 7.16\,\%$, $x^2 = 2.20$) and $Y_{1.992}Bi_{0.008}O_{2.90}$ ($R_{wp} = 7.10\,\%$, $x^2 = 2.62$) for the S48 and S192 samples, respectively, which are very close to those obtained from the thermogravimetric analysis. These consistent results imply that the amount of oxygen vacancies in the reduced phases is quite small.

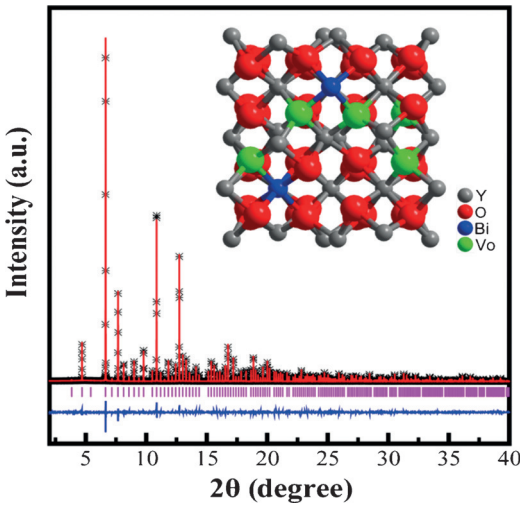

Figure 2. Rietveld fit to the high-resolution synchrotron XRD pattern of the S192 sample. The solid lines and overlying crosses show the calculated and observed intensities, respectively. The pink lines indicate the positions of the calculated Bragg reflections. The difference between the observed and calculated profiles is shown in blue. Inset: the structure of Bi-doped yttria with oxygen vacancies.

The existence of randomly distributed oxygen vacancies in the yttria inevitably alters the coordination environments and oxidation states of the Bi centers. If we assume one oxygen atom is extracted from the apical site of the [BiO_6] octahedra, the bond valence sum calculations give lower valences of Bi atoms with respect to those in the precursor (Figure S9). To unambiguously resolve the oxidation state and local environment of Bi, the X-ray absorption near-edge structure (XANES) and extended X-ray absorption fine structure (EXAFS) spectra were collected from the Bi L_{III} edge of the precursor and the S192 product; Bi metal and Bi_2O_3 powders were used as reference materials (Figure 3). Clearly, the Bi L_{III} edge of the precursor is similar to that of Bi_2O_3, indicating that Bi has a valence of +3. However, the Bi L_{III} edge of the S192 sample is located between those of Bi metal and Bi_2O_3, providing strong evidence for the emergence of Bi having an oxidation state between 0 and +3 (Figure 3a). Figure 3b shows the Fourier transforms (FTs) of the EXAFS at the Bi sites. The peaks in the *R* space correspond to

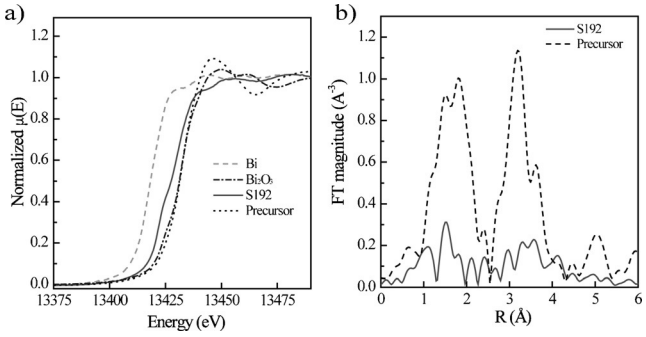

Figure 3. a) Bi L_{III}-edge XANES spectra of the precursor, Bi metal, Bi_2O_3, and the S192 sample. b) Fourier transforms (FTs) of the EXAFS spectra for the precursor and the S192 sample.

interatomic distances between absorbing and surrounding atoms. As a result of the photoelectron phase shift, all peaks in the FTs are shifted towards lower distances relative to the actual interatomic distances. The peak intensity is associated with the average number of neighbors of a given type and its mean square bond length disorder. We note that the S192 sample has a much weaker amplitude for all peaks relative to the precursor, implying a decreased number of neighboring atoms and significant disorder at the Bi site in the reduced phase. Interestingly, XANES and EXAFS analyses suggest that the local environment of Y is also slightly influenced by the oxygen de-intercalation (Figure S10), further evidencing that oxygen vacancies are randomly distributed in the yttria matrix.

Based on this combined body of experimental evidence, we concluded that the topochemical reduction leads to the evolution of [BiO_6] octahedra in $Y_{1.992}Bi_{0.008}O_3$ to [BiO_{6-z}] ($z < 6$) polyhedra in reduced phases, resulting in a reduction in the average oxidation states of Bi present. The reason for the systematic manipulation of emission behaviors is the formation of randomly distributed oxygen vacancies acting as ion-migration channels in the matrix. Such a low-temperature strategy avoids the formation of any Bi metal aggregates which generally occur in Bi-doped materials synthesized by means of high-temperature reactions.[21,23a] As a consequence, the emergence of NIR PL can be readily connected with Bi in the [BiO_{6-z}] units. With an increasing duration of CaH_2 treatment, the emission intensity from Bi^{3+} in the S_6 site gradually decreases and is weaker relative to the precursor (Figure 1), evidencing that the amount of [BiO_6] polyhedra with S_6 symmetry decreases. Note that the visible PL of Bi^{3+} in the C_2 site for the S12 sample is stronger than that of the precursor, probably because a small amount of oxygen vacancies is favorable to achieve high-efficiency emission for Bi^{3+} at this site (which does not have inversion symmetry); further extending the duration of CaH_2 treatment leads to emission of weaker intensity resulting from the decreased amount of Bi^{3+} present. It is found that all reduced phases demonstrate ultra-broad NIR emission profiles (Figure 1b; Figure S6, S7), which could be deconvoluted into two curves when photo-pumped by light at $\lambda = 614$ nm (Figure S11). 2D excitation–emission graphs unambiguously revealed that the reduced phases bear two classes of NIR-active centers with emission bands at circa $\lambda = 950$ and 1220 nm, corresponding to excitation at about $\lambda = 500/640$ and 610 nm, respectively (Figure S6). The energy transfer between two types of centers occurs owing to the overlapping of the excitation and emission bands. Both the excitation and emission bands for the reduced samples display a dependence on the treatment duration (that is, the number of oxygen vacancies; Figure S12), evidencing that there are some slight differences in the local environments of such NIR-active emitters. This is further supported by the time-resolved PL (Figure S13, S14). PL results clearly indicated the S48 sample is the most strongly emissive in the NIR region among all samples measured (Figure S7), suggesting that a moderate number of oxygen vacancies are of key for strong emission. This can be understood on the basis that the PL intensity is governed by the amount, quantum efficiency, and absorption cross-section

of the emitter. Unfortunately, at present it is still hard to determine the exact nature of the NIR-active centers observed,[20,21] although it is clear that such centers are closely connected with the $[BiO_{6-z}]$ units that are topotactically converted from the $[BiO_6]$ octahedra with S_6 and C_2 symmetries. Further work is under way to clarify this issue.

Additionally, we have found that this low-temperature topochemical reduction strategy can be readily extended to the manipulation of PL from other classes of Bi-doped compounds. For instance, after topochemical reduction by CaH_2, the visible emissions from Bi^{3+}-doped $LaGaO_3$, La_2O_3, and $LaAlO_3$ shift to NIR spectral ranges (Figure S15–S17). We believe that oxygen-deficient Bi–O polyhedra give rise to these emission profiles. The difference in the NIR PL characteristics for all reduced phases studied should result from different local environments of low-valence Bi in the materials.

To summarize, we have shown that the low-temperature topochemical reduction strategy can be employed as a powerful method for the synthesis of unconventional phosphors with luminescence covering the biological and/or telecommunication optical windows. Systematic characterization, including thermogravimetric, MS, synchrotron XRD, XANES, EXAFS, and PL analyses lead us to conclude that the topochemical treatment of $Y_{2-x}Bi_xO_3$ using CaH_2 results in the change of the valence of Bi to lower oxidation states as a result of the creation of randomly distributed oxygen vacancies. The change of Bi coordination environments from that in the $[BiO_6]$ octahedra in $Y_{2-x}Bi_xO_3$ to the oxygen-deficient $[BiO_{6-z}]$ polyhedra in reduced phases is the reason for the shift of the PL band maxima from the visible to the NIR spectral region. To the best of our knowledge, this is the first report on the rational manipulation of PL from typical Bi^{3+} emitters to those emitting in the NIR region, greatly deepening the understanding of Bi-related photophysical behavior. Importantly, we highlight this approach as a sufficiently general route for the manipulation of PL in other compounds, thereby opening up new avenues to develop novel luminescent systems that may be promising for a diverse array of functional applications. We anticipate that this low-temperature topochemical route can be extended to tune the properties of other types of optoelectronic materials.

Acknowledgements

This work is financially supported by the National Natural Science Foundation of China (Grant Nos. 11574225, 51472162, and U1532120), the Jiangsu Specially Appointed Professor program (Grant No. SR10900214), the Natural Science Foundation of Jiangsu Province for Young Scholars (BK20140336), a project funded by the Priority Academic Program Development of Jiangsu Higher Education Institutions (PAPD), and the Youth Project of National Natural Science Fund (11405256). The Spring-8 experiments were carried out with the approval of the Japan Synchrotron Radiation Research Institute (JASRI; Proposal No. 2015B0074). We are grateful to the staff at the 1W2B beamline at the Beijing Synchrotron Radiation Facility for XAFS measurements. We also thank the staff at the BL14W1 beamline at the Shanghai Synchrotron Radiation Facility for XAFS measurements.

Keywords: bismuth · luminescence · phosphors · reduction · topochemistry

How to cite: *Angew. Chem. Int. Ed.* **2016**, *55*, 4967–4971
Angew. Chem. **2016**, *128*, 5051–5055

[1] M. A. Hayward, M. A. Green, M. J. Rosseinsky, J. Sloan, *J. Am. Chem. Soc.* **1999**, *121*, 8843–8854.
[2] M. A. Hayward, M. J. Rosseinsky, *Chem. Mater.* **2000**, *12*, 2182–2195.
[3] M. A. Hayward, E. J. Cussen, J. B. Claridge, M. Bieringer, M. J. Rosseinsky, C. J. Kiely, S. J. Blundell, I. M. Marshall, F. L. Pratt, *Science* **2002**, *295*, 1882–1884.
[4] C. A. Bridges, G. R. Darling, M. A. Hayward, M. J. Rosseinsky, *J. Am. Chem. Soc.* **2005**, *127*, 5996–6011.
[5] Y. Tsujimoto, C. Tassel, N. Hayashi, T. Watanabe, H. Kageyama, K. Yoshimura, M. Takano, M. Ceretti, C. Ritter, W. Paulus, *Nature* **2007**, *450*, 1062–1065.
[6] M. O'Malley, M. A. Lockett, M. A. Hayward, *J. Solid State Chem.* **2007**, *180*, 2851–2858.
[7] H. Kageyama, T. Watanabe, Y. Tsujimoto, A. Kitada, Y. Sumida, K. Kanamori, K. Yoshimura, N. Hayashi, S. Muranaka, M. Takano, M. Ceretti, W. Paulus, C. Ritter, G. André, *Angew. Chem. Int. Ed.* **2008**, *47*, 5740–5745; *Angew. Chem.* **2008**, *120*, 5824–5829.
[8] J. Seddon, E. Suard, M. A. Hayward, *J. Am. Chem. Soc.* **2010**, *132*, 2802–2810.
[9] R. M. Helps, N. H. Rees, M. A. Hayward, *Inorg. Chem.* **2010**, *49*, 11062–11068.
[10] S. Tominaka, Y. Tsujimoto, Y. Matsushita, K. Yamaura, *Angew. Chem. Int. Ed.* **2011**, *50*, 7418–7421; *Angew. Chem.* **2011**, *123*, 7556–7559.
[11] Y. Kobayashi, O. J. Hernandez, T. Sakaguchi, T. Yajima, T. Roisnel, Y. Tsujimoto, M. Morita, Y. Noda, Y. Mogami, A. Kitada, M. Ohkura, S. Hosokawa, Z. Li, K. Hayashi, Y. Kusano, J. Kim, N. Tsuji, A. Fujiwara, Y. Matsushita, K. Yoshimura, K. Takegoshi, M. Inoue, M. Takano, H. Kageyama, *Nat. Mater.* **2012**, *11*, 507–511.
[12] a) A. M. Arévalo-López, J. A. Rodgers, M. S. Senn, F. Sher, J. Farnham, W. Gibbs, J. P. Attfield, *Angew. Chem. Int. Ed.* **2012**, *51*, 10791–10794; *Angew. Chem.* **2012**, *124*, 10949–10952; b) H. Jeen, W. S. Choi, J. W. Freeland, H. Ohta, C. U. Jung, H. N. Lee, *Adv. Mater.* **2013**, *25*, 3651–3656.
[13] T. Yamamoto, H. Kageyama, *Chem. Lett.* **2013**, *42*, 946–953.
[14] C. Tassel, L. Seinberg, N. Hayashi, S. Ganesanpotti, Y. Ajiro, Y. Kobayashi, H. Kageyama, *Inorg. Chem.* **2013**, *52*, 6096–6102.
[15] F. Denis Romero, S. J. Burr, J. E. McGrady, D. Gianolio, G. Cibin, M. A. Hayward, *J. Am. Chem. Soc.* **2013**, *135*, 1838–1844.
[16] F. Denis Romero, A. Leach, J. S. Möler, F. Foronda, S. J. Blundell, M. A. Hayward, *Angew. Chem. Int. Ed.* **2014**, *53*, 7556–7559; *Angew. Chem.* **2014**, *126*, 7686–7689.
[17] M. A. Hayward, *Semicond. Sci. Technol.* **2014**, *29*, 064010.
[18] a) T. Yamamoto, R. Yoshii, G. Bouilly, Y. Kobayashi, K. Fujita, Y. Kususe, Y. Matsushita, K. Tanaka, H. Kageyama, *Inorg. Chem.* **2015**, *54*, 1501–1507; b) G. Kaur Behrh, H. Serier-Brault, S. Jobic, R. Gautier, *Angew. Chem. Int. Ed.* **2015**, *54*, 11501–11503; *Angew. Chem.* **2015**, *127*, 11663–11665.
[19] T. Yajima, F. Takeiri, K. Aidzu, H. Akamatsu, K. Fujita, W. Yoshimune, M. Ohkura, S. Lei, V. Gopalan, K. Tanaka, C. M. Brown, M. A. Green, T. Yamamoto, Y. Kobayashi, H. Kageyama, *Nat. Chem.* **2015**, *7*, 1017–1023.

[20] a) G. Blasse, A. Bril, *J. Chem. Phys.* **1967**, *47*, 1920 – 1926; b) G. Blasse, A. Meijerink, J. Zuidema, *J. Phys. Chem. Solids* **1994**, *55*, 171 – 174.
[21] H.-T. Sun, J. J. Zhou, J. R. Qiu, *Prog. Mater. Sci.* **2014**, *64*, 1 – 72.
[22] a) E. M. Dianov, *Light: Sci. Appl.* **2012**, *1*, e12; b) H.-T. Sun, J. Yang, M. Fujii, Y. Sakka, Y. Zhu, T. Asahara, N. Shirahata, M. Ii, Z. Bai, J. Li, H. Gao, *Small* **2011**, *7*, 199 – 203; c) M. Ruck, *Angew. Chem. Int. Ed.* **2001**, *40*, 1182 – 1193; *Angew. Chem.* **2001**, *113*, 1222 – 1234; d) H.-T. Sun, Y. Sakka, H. Gao, Y. Miwa, M. Fujii, N. Shirahata, Z. Bai, J. Li, *J. Mater. Chem.* **2011**, *21*, 4060 – 4063; e) H.-T. Sun, Y. Sakka, N. Shirahata, H. Gao, T. Yonezawa, *J. Mater. Chem.* **2012**, *22*, 12837 – 12841; f) H.-T. Sun, T. Yonezawa, M. M. Gillett-Kunnath, Y. Sakka, N. Shirahata, S. Gui, M. Fujii, S. C. Sevov, *J. Mater. Chem.* **2012**, *22*, 20175 – 20178; g) H.-T. Sun, Y. Matsushita, Y. Sakka, N. Shirahata, M. Tanaka, Y. Katsuya, H. Gao, K. Kobayashi, *J. Am. Chem. Soc.* **2012**, *134*, 2918 – 2921; h) S. Ulvenlund, L. Bengtsson-Kloo, *J. Chem. Soc. Faraday Trans.* **1995**, *91*, 4223 – 4234.
[23] a) Y. Fujimoto, M. Nakatsuka, *Jpn. J. Appl. Phys.* **2001**, *40*, L279 – L281; b) V. O. Sokolov, V. G. Plotnichenko, E. M. Dianov, *Opt. Mater. Express* **2014**, *5*, 163 – 168; c) O. Laguta, H. E. Hamzaoui, M. Bouazaoui, V. B. Arion, I. Razdobreev, *Opt. Lett.* **2015**, *40*, 1591 – 1594; d) B. B. Xu, S. F. Zhou, D. Z. Tan, Z. L. Hong, J. H. Hao, J. R. Qiu, *J. Appl. Phys.* **2013**, *113*, 083503.
[24] a) L. S. Chi, R. S. Liu, B. J. Lee, *J. Electrochem. Soc.* **2005**, *152*, J93 – J98; b) F. Réal, B. Ordejón, V. Vallet, J. Flament, J. Schamps, *J. Chem. Phys.* **2009**, *131*, 194501.
[25] A. C. Larson, R. B. Von Dreele, Los Alamos National Laboratory Report LAUR 86-748, **2000**.

Received: February 2, 2016
Published online: March 11, 2016

